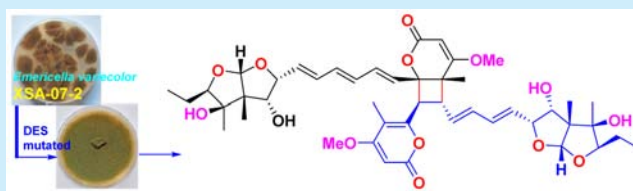


Diasteltoxins A–C, Asteltoxin-Based Dimers from a Mutant of the Sponge-Associated *Emericella varicolor* FungusHailin Long,[†] Zhongbin Cheng,[†] Wei Huang,[†] Qi Wu,[†] Xiaodan Li,[†] Jingrong Cui,[†] Peter Proksch,[‡] and Wenhan Lin^{*,†}[†]State Key Laboratory of Natural and Biomimetic Drugs, Peking University, Beijing 100191, P. R. China[‡]Institute of Pharmaceutical Biology and Biotechnology, Heinrich-Heine University, 40225 Duesseldorf, Germany

S Supporting Information

ABSTRACT: Three novel asteltoxin-bearing dimers namely diasteltoxins A–C (1–3) along with asteltoxin were isolated from a mutated strain of a sponge-derived fungus *Emericella varicolor* XSA-07-2. Their structures were determined by extensive spectroscopic analyses including the computed electronic circular dichroism (ECD) data for the configurational assignment. The biogenetic formation of the dimers through [2 + 2] cycloaddition of asteltoxin was postulated. Diasteltoxins 1–3 exerted inhibitory effects against the tumor cell lines H1299 and MCF7 and exhibited significant inhibition against thioredoxin reductase (TrxR).



Marine-derived microorganisms have been proven as a promising source to produce structurally novel natural products which play a pivotal role in the development of new therapeutics.^{1–4} It was recognized that most biosynthetic pathways of marine microbial strains keep silent under standard laboratory culture approaches, and chemists are only scratching the surface of biosynthetic diversity due to the absence of particular stimuli.⁵ Thus, it is a challenge to uncover the true biosynthetic potential of these diverse microorganisms. Indeed, several approaches have been developed to intentionally awaken the silent biosynthetic pathways to access cryptic compounds,^{6–8} including the strategies of OSMAC (one strain many compounds),⁹ cocultivation, ribosome engineering,^{10,11} and chemical epigenetics methods.^{12,13} In addition, introducing drug-resistant mutation¹⁴ and random diethyl sulfate (DES) mutagenesis¹⁵ also provided exciting opportunities to harness the biosynthetic potential of known and cultivable microorganisms. Asteltoxin is a mycotoxin originally derived from fungus *Aspergillus stellatus*, and its structure is related to trienic α -pyrone characterized by the presence of a unique and highly functionalized dioxabicyclooctane bearing an array of six stereogenic centers.^{16–18} Asteltoxin possesses a range of biological activities, including the potent inhibition against bacterial ATP-synthesis and ATP-hydrolysis catalyzed by mitochondria enzyme systems. The biosynthetic pathway to form asteltoxin and relative analogues was uncovered by ¹³C-labeled precursor studies¹⁹ and by the biosynthetic gene cluster and its reconstitution using heterologous expression.²⁰ Our previous investigation of a sponge-associated fungus *Emericella varicolor* XSA-07-2 resulted in the isolation of asteltoxin as a main metabolite in addition to a number of polyketides.²¹ In the continuing discovery of new metabolites, we applied diethyl sulfate (DES) as the chemical mutagen to activate the silent

fungal metabolite pathway of *E. varicolor*. Eight mutated strains were obtained, while the HPLC, NMR, and ESIMS/MS detection revealed that a mutant of *E. varicolor* XSA-07-2-M3 produced the secondary metabolites structurally featured asteltoxin, which were not found in the wild strain. Chromatographic separation of the fermented mutant resulted in the isolation of three new compounds namely diasteltoxins A–C (1–3) (Figure 1) together with asteltoxin.

Diasteltoxin A (1) was isolated as a white amorphous powder. Its molecular formula was determined as C₄₆H₆₀O₁₄ on the basis of the pseudomolecular ion peak at m/z 837.4058 [$M + H$]⁺ (calcd for C₄₆H₆₁O₁₄, 837.4061) in the HRESIMS and NMR data, requiring 17 degrees of unsaturation. The UV absorptions at 243 and 295 nm in association with the IR data at 3418, 1716, and 1619 cm^{−1} suggested the presence of hydroxy, lactone, and olefinic functionalities. The ¹³C NMR spectrum exhibited a total of 46 carbon resonances, including two carbonyl carbons, 16 olefinic carbons for eight double bonds, two methoxy carbons, and a number of oxygenated and alkyl carbons. The ¹H and ¹³C NMR data (Table 1 in the Supporting Information) featured an asteltoxin-type analogue, while the 2D NMR (COSY, HMQC, HMBC) data established two units of asteltoxin related moieties. In unit A, a conjugated olefinic chain from H-9 (δ_H 5.86, dd, J = 7.8, 15.6 Hz) to H-14 (6.00, d, J = 15.6 Hz) established a triene segment. A dioxabicyclooctane moiety was assigned by the COSY correlation between H-7 (δ_H 3.54, dd, J = 3.6, 6.0 Hz)/H-8 (δ_H 4.46, dd, J = 3.6, 7.2 Hz) and H-8/H-9, in association with the HMBC correlations from proton singlet H-6 (δ_H 5.00, s) to the carbons in the bicyclic ring from C-3 (δ_C 89.3) to C-8 (δ_C

Received: August 4, 2016

Published: August 29, 2016

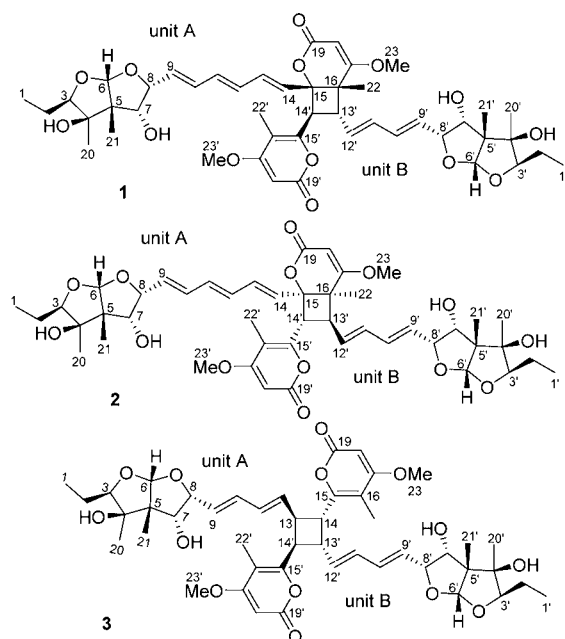


Figure 1. Structures of diasteltoxins A–C (1–3).

Table 1. Inhibitory Effects of 1–3 Against Tumor Cell Lines and TrxR

compd	IC ₅₀ (μM)			TrxR
	HEK293T	H1299	MCF7	
1	132	188	73	12.8 ± 0.8
2	102	164	127	11.1 ± 0.2
3	79	142	50	7.2 ± 0.2

84.5). Additional HMBC correlations from H₃-20 (δ_{H} 1.18, s) to C-3, C-4 (δ_{C} 79.8), and C-5 (δ_{C} 61.6), H₃-21 (δ_{H} 1.01, s) to C-4, C-5, C-6 (δ_{C} 111.9), and C-7 (δ_{C} 78.9), and H₃-1 to C-3, in association with the COSY correlations from H₃-1 (δ_{H} 0.89, t, J = 7.2 Hz) to H-3 (δ_{H} 4.15, t, J = 6.0 Hz) for a propane group, indicated the partial structure of unit A from C-1 to C-14 to be identical to that of asteltoxin. However, the HMBC correlations from H-14 to C-15 (δ_{C} 83.6) and C-16 (δ_{C} 49.4), between MeO and C-17 (δ_{C} 174.2), and H₃-22 (δ_{H} 1.25, s) to C-15, C-16, and C-17, in addition to the correlations from H-18 (δ_{H} 5.47, s) to C-16, C-17, and C-19 (δ_{C} 163.5), revealed C-15/C-16 of the α -pyrone unit to be saturated. Following the spectroscopic analyses as in the case for unit A, the structure of unit B was established to be closely related to asteltoxin. The distinction was attributed to the side chain, where C-13' (δ_{C} 43.5) and C-14' (δ_{C} 50.3) presented as sp³ hybridization instead of olefinic carbons as in asteltoxin. This assignment was also supported by the COSY relationships from H-13' (δ_{H} 3.32, dd, J = 8.4, 10.8 Hz) to H-12' (δ_{H} 5.60, dd, J = 8.4, 15.6 Hz) and H-14' (δ_{H} 4.03, d, J = 10.8 Hz). The linkage of the 16'-methyl-17'-methoxy- α -pyrone to C-14' was deduced by the HMBC correlations of H-14' to C-15' and C-16'. The connection of units A and B across C-14'/C-15 and C-13'/C-16 was deduced by the HMBC correlations between H₃-22 and C-13' and between H-14 and C-14'. Thus, the structure of 1 was deduced as a dimer of asteltoxin through [2 + 2] cycloaddition. The relative configurations of 1 were determined by the NOESY interaction. The observation of NOE interactions between H₃-20/H-3 and H₃-20'/H-3', as well as H₃-21 to H₂-2, H-6, H-7, and H-8, as well as H₃-21' to H₂-2',

H-6', H-7', and H-8', clarified the relative configurations of both dioxabicyclooctane moieties in units A and B to be the same as those of asteltoxin, which was also isolated from the same fraction. In addition, the *E* geometry of the double bonds at side chains was assigned by the coupling constants of the olefinic protons. Since the relative configurations of asteltoxin were determined by spectroscopic data and X-ray analyses¹⁷ and its absolute configurations were assigned by partial²² and total synthesis,²³ the configurations of units A and B were biogenetically presumed to be the same as those of the known analogue. Regarding the cyclobutane ring, the strong NOE correlation between H-12' and H-14', and from H₃-22 to H-13' and H-14, determined the *cis* fusion of unit A with unit B, while H-13' was in the same orientation as H₃-22 and in the opposite one to H-14' (Figure 2). These data afforded the relative

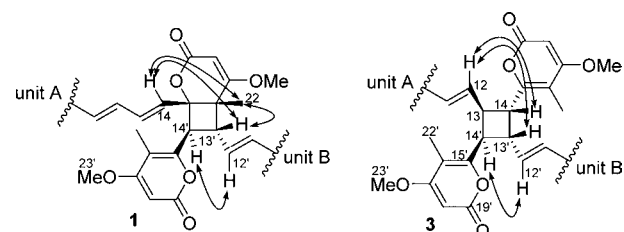


Figure 2. Key NOE correlations of 1 and 3 in cyclobutane ring.

configurations of 1 to be 15*S**, 16*S**, 13'*R**, and 14'*S**. In the ECD spectrum, compound 1 exhibited a negative Cotton effect (CE) at 305 nm and positive CE at 255 nm (Figure 3),

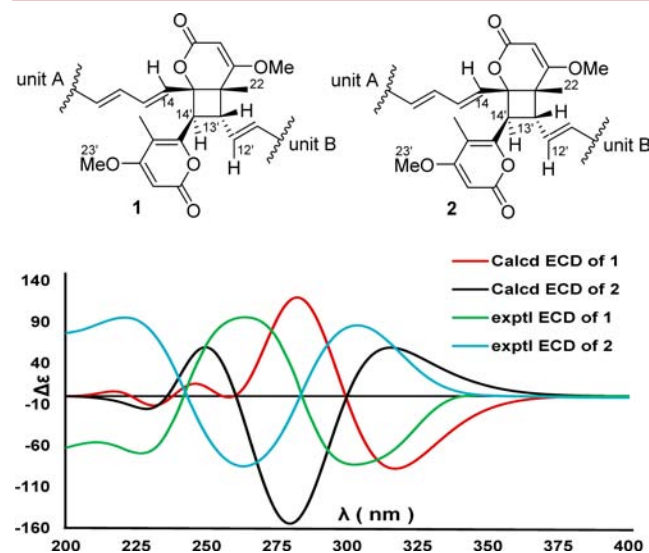


Figure 3. Experimental ECD spectra of 1 and 2 and the calculated spectra of 1 and 2.

reflecting the exciton coupling of α -pyrones in units A and B. These data were in accordance with the negative chirality helicity,²⁴ indicating 14'*S* configuration. Thus, the remaining stereogenic centers in the cyclobutane ring were assigned as 15*S*, 16*S*, and 13'*R*, accordingly. These assignments were also supported by a quantum chemical ECD calculation. Conformational searches were carried out by means of the Powell methods using the MMFF94s force field in the SYBYL-X software package.²⁵ The corresponding minimum geometries were fully optimized at the B3LYP/6-31G(d) level using the

time-dependent density functional theory (TDDFT) method, as implemented in the Gaussian 09 program package. The stable conformers obtained were then submitted to the ECD calculation at the B3LYP/6-31G(d) level. The calculated ECD spectra of the model molecules with 15S, 16S, 13'R, and 14'S (**1**) and 15R, 16R, 13'S, and 14'R configurations (**2**) were subsequently compared with the experimental ECD data for **1**. The similar Cotton effects of the measured ECD of **1** as those of computed **1** confirmed the configurational assignments.

The molecular formula of diasteltoxin B (**2**) was the same as that of **1** based on the HRESIMS and NMR data, while the UV and IR absorptions of both compounds were closely similar. An extensive analyses of 1D and 2D (COSY, HSQC, HMBC) NMR data revealed the same gross structure of both **2** and **1**. The NOE data and the coupling constants of units A and B in **2** resembled those **1**, indicating **2** shared the same configurations of asteltoxin. In addition, the NOE correlation between H-14 and H₃-22 deduced a *cis* fusion of unit A with unit B, while the NOE relationships between H₃-22/H-13' and H-12'/H-14' revealed the same relative configurations in the cyclobutane ring of both **1** and **2**. However, the ECD spectrum exhibited the positive CE at 310 nm and negative CE at 260 nm, which were in opposite phases in comparison with those of **1**. Since the CEs were mainly contributed to by α -pyrone chromophores substituted in the cyclobutane ring, the Cotton effects of **2** were in agreement with 14'R configuration, based on the exciton chirality method. These assignments were further supported by the experimental ECD data which resembled the computed ECD data (Figure 3) for the model molecule of **2** with 15R, 16R, 13'S, and 14'R configurations.

Diasteltoxin C (**3**) has a molecular formula the same as that of **1**, as determined by the HRESIMS and NMR data. The similar UV and IR absorptions and NMR data for both **3** and **1** indicated **3** to be an analogue of **1**. Comprehensive analyses of 2D NMR data including COSY, HMQC, and HMBC revealed the structure of **3** to be a dimer of asteltoxin with the saturated carbons of C-13 (δ_C 41.2)/C-14 (δ_C 42.8) in unit A and C-13' (δ_C 41.4)/C-14' (δ_C 43.2) in unit B. These findings were supported by the key HMBC correlations from H-14 (δ_H 3.86, dd, J = 6.8, 9.8 Hz) to C-12', C-13', and C-14' and from H-14' to C-12, C-13, and C-14, in association with the COSY relationships of the protons surrounding the cyclobutane ring. Thus, the gross structure of **3** was determined as a dimer of asteltoxin with a [2 + 2] cycloaddition through C-13/C-14' and C-14/C-13' condensation. The NOE correlations from H-12 to H-14 and H-13' and from H-12' to H-14' and H-13 established the same orientation of H-14 and H-13' which were on the opposite face toward H-13 and H-14'. Therefore, the relative configuration of cyclobutane was assigned as 13R*, 14R*, 13S*, and 14S*. Based on the quantum chemical ECD calculation at the B3LYP/6-31G+(d) level using the TDDFT method, the ECD data for the model molecules for 13R, 14R, 13'S, and 14'S (**3a**) and 13S, 14S, 13'R, and 14'R (**3b**) (Figure 4) were computed. Comparison of the experimental ECD of **3** with those calculated for the model molecules clarified **3** to be in 13R, 14R, 13'S, and 14'S configurations.

Biogenetically, compounds **1** and **2** were postulated to be derived from two units of asteltoxin as a precursor through [2 + 2] cycloaddition, while the *E* geometry of the double bond at C-13'/C-14' of the second asteltoxin resulted in the *trans* orientation of H-13' and H-14'. Two fusion manners were depicted to generate **1** and **2**, respectively. Compound **3** was generated by the condensation of asteltoxin through [2 + 2]

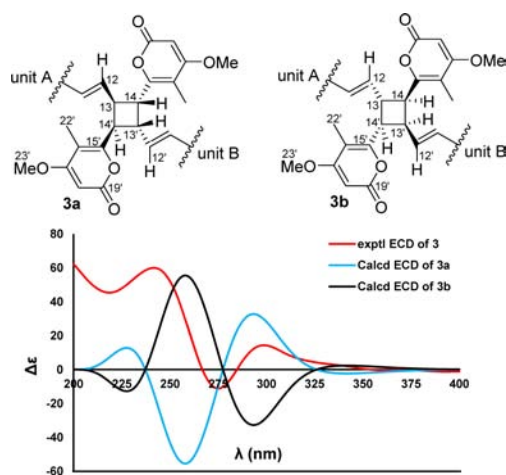


Figure 4. Experimental ECD spectrum of **3** and the calculated spectra of **3a** and **3b**.

cycloaddition across C-13/C-14' and C-14/C-13' (Figure 5). Phytochemical reaction of asteltoxin under irradiation with a

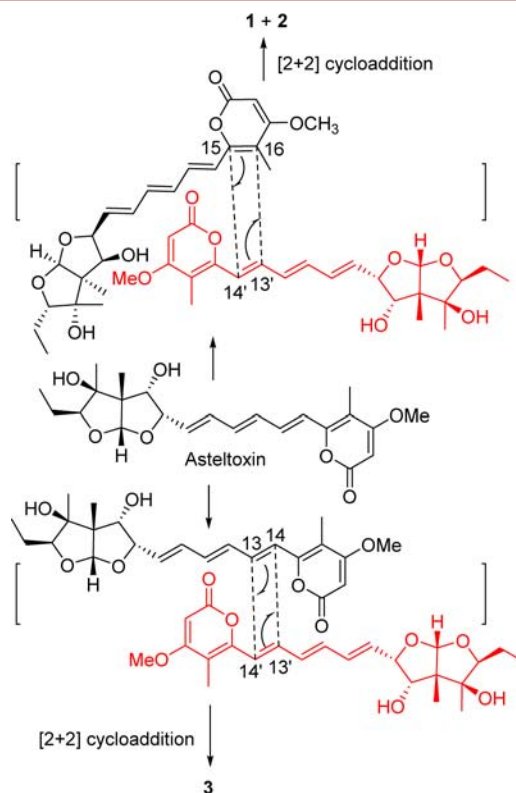


Figure 5. Plausible biogenetic pathway of **1**–**3**.

400 W medium-pressure mercury lamp for 1.0 h was performed,³³ while no product regarding **1**–**3** was detected. This finding partly supported **1**–**3** as being derived from fungal origin.

Diasteltoxins A–C (**1**–**3**) exerted weak inhibitory effects against the growth of nonsmall cell lung cancer (H1299) and breast cancer (MCF7) cell lines, whereas compounds **1**–**3** exhibited significant inhibition against thioredoxin reductase (TrxR) (Table 1). TrxR is a member of the Trx system and is regarded as a new target for anticancer drug development due to its overexpression in many aggressive tumors. In addition,

TrxR has been proven to be closely related to tumor progression and metastasis *in vivo*.²⁶ Thus, the weak cytotoxicity and potent inhibition toward TrxR suggested that diasteltoxins A–C may act as microenvironmental regulation of tumor progression and metastasis.

In summary, the present work reports three structurally novel asteltoxin-bearing dimers which were characteristic of a [2 + 2] cycloaddition of asteltoxin in different manners. Naturally occurring dimers with [2 + 2] cycloaddition are a group of unusual metabolites in nature, while they were mainly found from plants as exemplified by simmonosides A and B,²⁷ katsumadain C,²⁸ oxyfadichalcones A–C, achyrodimers A–E,²⁹ and grahamines A–E.³⁰ Photodimerization to form a cyclobutane ring was proposed tentatively by the plants irradiated under intense ultraviolet light in their growing environment. Marine organisms rarely exhibited dimerization through [2 + 2] cycloaddition with the exception of debromosceptrins from the sponge *Agelas conifer*³¹ and pulchralides from macroalgae.³² To the best of our knowledge, this is the first report of [2 + 2] cycloaddition occurring in marine fungus, while the dimerization was suggested to be accomplished by an enzymatic step due to the unsuccessful dimerization of asteltoxin in a photochemical reaction.

■ ASSOCIATED CONTENT

Supporting Information

The Supporting Information is available free of charge on the ACS Publications website at DOI: 10.1021/acs.orglett.6b02313.

NMR, HSQC, HMBC, COSY, NOESY, HRESIMS, UV, and IR spectral data (PDF)

■ AUTHOR INFORMATION

Corresponding Author

*E-mail: whlin@bjmu.edu.cn.

Notes

The authors declare no competing financial interest.

■ ACKNOWLEDGMENTS

This work was supported by grants from the 973 program (2015CB755906), NSFC-Shangdong Join Fund for Marine Science (U1406402), and NSFC (81630089, 41376127).

■ REFERENCES

- (1) Hertweck, C. *Nat. Chem. Biol.* **2009**, *5*, 450–452.
- (2) Newman, D. J.; Cragg, G. M. *Mar. Drugs* **2014**, *12*, 255–278.
- (3) Blunt, J. W.; Copp, B. R.; Keyzers, R. A.; Munro, M. H. G.; Prinsep, M. R. *Nat. Prod. Rep.* **2014**, *31*, 160–258.
- (4) Newman, D. J.; Cragg, G. M. *J. Nat. Prod.* **2007**, *70*, 461–477.
- (5) Brakhage, A. A.; Schroeckh, V. *Fungal Genet. Biol.* **2011**, *48*, 15–22.
- (6) Zerikly, M.; Challis, G. L. *ChemBioChem* **2009**, *10*, 625–633.
- (7) Gross, H. *Curr. Opin. Drug Discovery Dev.* **2009**, *12*, 207–219.
- (8) Scherlach, K.; Hertweck, C. *Org. Biomol. Chem.* **2009**, *7*, 1753–1760.
- (9) Bode, H. B.; Bethe, B.; Höfs, R.; Zeeck, A. *ChemBioChem* **2002**, *3*, 619–627.
- (10) Hosaka, T.; Ohnishi-Kameyama, M.; Muramatsu, H.; Murakami, K.; Tsurumi, Y.; Kodani, S.; Yoshida, M.; Fujie, A.; Ochi, K. *Nat. Biotechnol.* **2009**, *27*, 462–464.
- (11) Ochi, K. *Biosci., Biotechnol., Biochem.* **2007**, *71*, 1373–1386.
- (12) Cichewicz, R. H. *Nat. Prod. Rep.* **2010**, *27*, 11–22.
- (13) Wang, X.; Sena Filho, J. G.; Hoover, A. R.; King, J. B.; Ellis, T. K.; Powell, D. R.; Cichewicz, R. H. *J. Nat. Prod.* **2010**, *73*, 942–948.
- (14) Chai, Y. J.; Cui, C. B.; Li, C. W.; Wu, C. J.; Tian, C. K.; Hua, W. *Mar. Drugs* **2012**, *10*, 559–582.
- (15) Fang, S.; Cui, C.; Li, C.; Wu, C.; Zhang, Z.; Li, L.; Huang, X.; Ye, W. *Mar. Drugs* **2012**, *10*, 1266–1287.
- (16) Maebayashi, Y.; Suzuki, S.; Horie, Y.; Murai, T.; Yamazaki, M. *Mycotoxins* **1983**, *1983*, 47–49.
- (17) Kruger, G. J.; Steyn, P. S.; Vlegaar, R.; Rabie, C. J. *J. Chem. Soc., Chem. Commun.* **1979**, *10*, 441–442.
- (18) Eom, K. D.; Raman, J. V.; Kim, H.; Cha, J. K. *J. Am. Chem. Soc.* **2003**, *125*, 5415–5421.
- (19) Steyn, P. S.; Vlegaar, R. *J. Chem. Soc., Chem. Commun.* **1984**, *15*, 977–979.
- (20) Lin, T. S.; Chiang, Y. M.; Wang, C. C. *Org. Lett.* **2016**, *18*, 1366–1369.
- (21) Wu, Q.; Wu, C. M.; Long, H. L.; Chen, R.; Liu, D.; Proksch, P.; Guo, P.; Lin, W. *J. Nat. Prod.* **2015**, *78*, 2461–2470.
- (22) Schreiber, S. L.; Satake, K. *Tetrahedron Lett.* **1986**, *27*, 2575–2578.
- (23) Eom, K. D.; Raman, J. V.; Kim, H.; Cha, J. K. *J. Am. Chem. Soc.* **2003**, *125*, 5415–5421.
- (24) Cai, G.; Bozhkova, N.; Odingo, J.; Berova, N.; Nakanishi, K. *J. Am. Chem. Soc.* **1993**, *115*, 7192–7198.
- (25) Li, Q.; Ren, J.; Zhou, B.; Bai, B.; Liu, X.; Wen, M.; Zhu, H. *Tetrahedron* **2013**, *69*, 3067–3074.
- (26) Lu, J.; Chew, E. H.; Holmgren, A. *Proc. Natl. Acad. Sci. U. S. A.* **2007**, *104*, 12288–12293.
- (27) Abdel-Mageed, W. M.; Bayoumi, S. A. L.; Al-wahaibi, L. H.; Li, L.; Sayed, H. M.; Abdelkader, M. S. A.; El-Gamal, A. A.; Liu, M.; Zhang, J.; Zhang, L.; Liu, X. *Org. Lett.* **2016**, *18*, 1728–1731.
- (28) Yang, C.; Wang, X.; Wang, J.; Luo, J.; Luo, J.; Kong, L. *Org. Lett.* **2011**, *13*, 3380–3383.
- (29) Sagawa, T.; Takaishi, Y.; Fujimoto, Y.; Duque, C.; Osorio, C.; Ramos, F.; Garzon, C.; Sato, M.; Okamoto, M.; Oshikawa, T.; Ahmed, S. U. *J. Nat. Prod.* **2005**, *68*, 502–505.
- (30) Cretton, S.; Bartholomeusz, T. A.; Humam, M.; Marcourt, L.; Allenbach, Y.; Jeannerat, D.; Munoz, O.; Christen, P. *J. Nat. Prod.* **2011**, *74*, 2388–2394.
- (31) Shen, X.; Perry, T. L.; Dunbar, C. D.; Kelly-Borges, M.; Hamann, M. T. *J. Nat. Prod.* **1998**, *61*, 1302–1303.
- (32) Ankisetty, S.; Nandiraju, S.; Win, H.; Park, Y. C.; Amsler, C. D.; McClintock, J. B.; Baker, J. A.; Diyabalanage, T. K.; Pasaribu, A.; Singh, M. P.; Maiese, W. M.; Walsh, R. D.; Zaworotko, M. J.; Baker, B. J. *J. Nat. Prod.* **2004**, *67*, 1295–1302.
- (33) The solution of asteltoxin (10.0 mg) in 1.5 mL of anhydrous dioxane was purged with N₂ for 10 min and irradiated with a 400 W medium-pressure mercury lamp under N₂ for 1.0 h. After irradiation, the solvent was removed *in vacuo*, while the residue was detected by TLC and HPLC with 3 as a reference sample.